



The Use of Geophysical Well Logs in Determining the Some Petrophysical Properties of the Bajawan Formation in Selected Wells from the Kirkuk Field, Northern Iraq

Farah M. Al-Mawla ¹ , Bashar A. Al-Juraisy ^{2*} , Rafee I. Al-Hamidi ³ , Qahtan M. Hussain ⁴

^{1,2,3}Department of Geology, College of Science University of Mosul, Mosul, Iraq.

⁴North Oil Company, Kirkuk, Iraq.

Article information

Received: 10- Apr -2023

Revised: 13- May -2023

Accepted: 29- May -2023

Available online: 31- Dec – 2023

Keywords:

Bajawan Formation
Petrophysics properties
Well logs
Kirkuk

Correspondence:

Name: Bashar A. Al-Juraisy

Email :

dr.bashar91967@gmail.com

ABSTRACT

The Kirkuk oil field is one of the Iraqi large and old oil fields, as it was produced in the thirties of the previous century (twentieth century). The production of oil for long periods may lead to a decrease in the pressure of the hydrocarbon flow inside the wells, which may require development operations for these wells, and these operations require sufficient knowledge of the petrophysical properties, of which is the porosity as the most important property of the rocks.

The main objective of this study is to evaluate the proportions and types of porosity within the rocks of the Bajawan Formation, which is considered one of the oil-producing Tertiary formations in the Kirkuk oil field.

In this study, twenty thin sections are examined as well as porosity logs are analyzed for three wells drilled in the Baba dome (K-183, K-218, and K-246). Baba dome is one of the three domes of the Kirkuk anticline.

The results of the study show that the proportion of porosity in the formation is relatively high, that there are multiple types of primary and secondary porosities, and that the effective porosity is close to the total porosity due to the low percentage of shale in the formation. The results of the study also show that there are some limited areas that may contain gas.

DOI: [10.33899/earth.2023.141399.1105](https://doi.org/10.33899/earth.2023.141399.1105), ©Authors, 2023, College of Science, University of Mosul.

This is an open access article under the CC BY 4.0 license (<http://creativecommons.org/licenses/by/4.0/>).

استخدام سجلات الآبار الجيوفيزيائية في تحديد بعض الخصائص البتروفيزيائية لتكوين باجوان في آبار مختارة من حقل كركوك / شمال العراق

فرح محمد المولى¹، بشار عزيز الجريسي²، رافع ابراهيم الحميدي³، قحطان محمد حسين⁴

^{1,2,3} قسم علوم الأرض كلية العلوم، جامعة الموصل، الموصل، العراق

⁴ شركة نفط الشمال، كركوك، العراق

المخلص	معلومات الارشفة
يعتبر حقل كركوك النفطي أحد حقول العراق النفطية الكبيرة والقديمة الانتاج، حيث بدأ الانتاج فيه منذ ثلاثينيات القرن العشرين، ولا يزال مستمرا الى وقتنا الحاضر.	تاريخ الاستلام: 10- ابريل -2023
ان انتاج النفط لفترات طويلة قد يؤدي الى انخفاض ضغط تدفق الهيدروكربون داخل الآبار مما قد نحتاج الى عمليات تطوير لتلك الآبار وهذه العمليات تحتاج معرفة كافية بالخصائص البتروفيزيائية واهمها مسامية الصخور.	تاريخ المراجعة: 13- مايو -2023
الهدف الاساس من هذه الدراسة هو تقييم نسب وانواع المسامية داخل صخور تكوين باجوان الذي يعتبر أحد تكاوين العصر الثلاثي المنتجة للنفط في حقل كركوك النفطي.	تاريخ القبول: 29- مايو -2023
في هذه الدراسة تم فحص عشرين شريحة مجهر، وكذلك تحليل سجلات المسامية لثلاثة آبار (K-183, K-218, K-246) محفورة في قبة بابا والتي هي احدى القباب الثلاث لطية كركوك المحدبة.	تاريخ النشر الالكتروني: 31- ديسمبر -2023
اوضحت نتائج الدراسة بان نسبة المسامية في التكوين عالية نسبيا، وان هنالك انواعاً متعددة من المسامية الاولية والثانوية، وان المسامية الفعالة كانت مقاربة للمسامية الكلية بسبب تدني نسبة السجيل في التكوين. كما اوضحت نتائج الدراسة ان هنالك بعض الأبنطة المحدودة ربما تحتوي على الغاز.	الكلمات المفتاحية: تكوين باجوان الخواص البتروفيزيائية سجلات الآبار كركوك
	المراسلة: الاسم: بشار عزيز الجريسي Email: dr.bashar91967@gmail.com

DOI: 10.33899/earth.2023.141399.1105, ©Authors, 2023, College of Science, University of Mosul.

This is an open access article under the CC BY 4.0 license (<http://creativecommons.org/licenses/by/4.0/>).

Introduction

Considering that the recoverable oil reserves in the Kirkuk oil field are estimated to be 8.7 trillion barrels, it can be considered that it is one of the largest oil fields in Iraq (Mehdi, 2018). The Bajawan Formation is one of the sequences of the Oligocene carbonate series that produces oil in the Kirkuk oil field, and its importance lies in the fact that production from it is still continuing to the present time. The formation age is middle Oligocene, and it was deposited along the northeast of the Oligocene basin. The most important formation's outcrops that appear in the Qara Chuq anticline, as for the subsurface sections, it is found in the wells of Kirkuk, Ain Zala and Bay Hassan (Bellen et al. 1959; Ditmar et al., 1971; Buday 1980).

The study of the petrophysical characteristics of oil-producing formations is very important in following up the developments of the post-production stages (Abdulaziz, et al. 2022) as well as the stages of well development (Khudhair and Al-Zaidy, 2018). One of the most important petrophysical characteristics that determine the characteristics of oil-producing formations is porosity and its types (Hou, et al, 2022), which conclusively determines the amount of hydrocarbon that can be extracted from the rocks, as well as the economic viability of the oil production process in the field.

The petrophysical properties are estimated in several ways, including direct methods by means of core and rock cutting which are costly and not comprehensive for all well depths, and indirect methods by estimating these properties by geophysical well logs.

There are many studies that used well logs data to determine the petrophysical characteristics of hydrocarbon-producing formations in Iraq, such as Al-Hamdany and Sulaiman (2014); Al-Majid (2019, 2021); Al-Juraisy and Al-Majid (2021); Mahdi and Farman (2023).

The aim of the current study is to determine the amount and types of porosity in the Bajawan carbonate Formation by analyzing the available well logs and rock cutting thin section for selected depths of the formation in the wells (K-183, K-218, K-246) within the dome of Baba from Kirkuk anticline and the possibility of the presence of gas in some parts of this formation.

Site description

The study area is located in the Kirkuk oil field near the city of Kirkuk in northeastern Iraq, where the field extends parallel to the northern and northwestern boundaries of the city (Fig. 1) In general, the Kirkuk oil field has a longitudinal, asymmetrical, boxy anticline with double plunging, and its axis extends in a northwest-southeast direction. It has a length of approximately 100 km and a width of 4 km. It is represented by three domes, namely the Khurmala dome at the northwestern end of the fold and the dome of Baba at the southeastern end of the fold and between them in the middle is the Avanah dome (Fig.1)

The study area is located within the unstable shelf and within the foothill tectonic division of Iraq (Fouad, 2015) as shown in the figure (2), which is characterized by the presence of longitudinal, narrow and asymmetrical anticlines (Jassim and Goff, 2006).

Bajawan Formation is described stratigraphically for the first time by Bellen at well K-109 (Bellen, 1956). It comprised thin argillaceous limestone beds with abundant coral fragments and tight back reef miliolid limestones that alternated with porous, partially dolomitized, rotalid-algal reef limestones (Jassim and Goff, 2006). Configuration of the door and from the top of the formation of the hole. Table (1) shows some details of the formation in the three wells of the study.

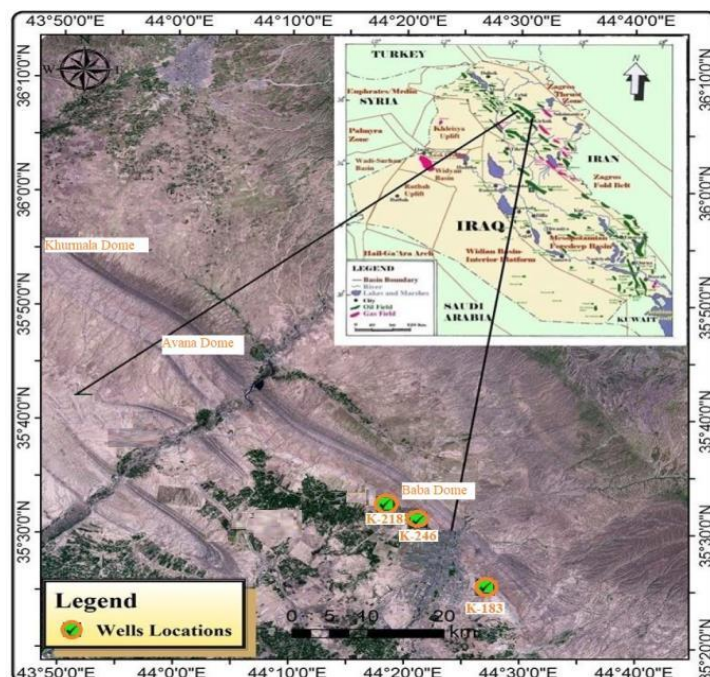


Fig. 1. Location map for studied area

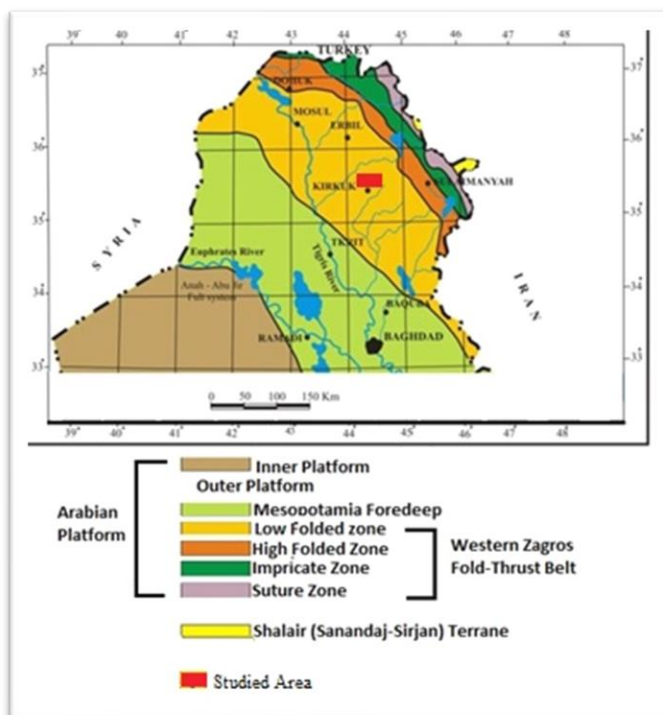


Fig. 2. Iraqi tectonic map (modified from Fouad, 2015)

Table 1: Locations and thicknesses of Bajawan Formation in studied wells

Wells	Top of formation (m)	Thickness (m)	Location	
			longitude	Latitude
K-183	871.7	20.1	44° 26' 51.97"	35° 25' 24.60"
K-218	403	18	44° 18' 21.33"	35° 32' 24.22"
K-246	328	55	44° 21' 28.13"	35° 31' 30.62"

Materials and Methods.

The study included two aspects, the first included an analysis of analogue well logs data, while the second included the preparation of thin section of cutting rocks samples and examining them under a microscope to diagnose the different types of porosity.

There are some analogue logs available for the three studied wells (K-183, K-218, K-246) as shown in the Table 2.

Table 2: available logs for studied wells

Well	Available well logs					
	Caliper	Gamma ray	Neutron	Density	photoelectric (PEF)	Sonic
K-183	*	*	*			*
K-218	*	*	*	*	*	*
K-246	*	*	*	*		*

*Available logs

The interpretation includes the lithology estimation, the percentage of different minerals types, and the volume of shale at all depths in the formation, as well as the percentage and types of different types of porosity.

In general, the interpretation processes that are performed on the well data can be summarized in the following stages:

- 1- Analogue data are converted to digital data for a set of available well logs for the three wells (K-183, K-218, K-246) using Didger® 3 Program in order to prepare them for well logs interpretation program (IP 3.5).
- 2- To perform environment corrections on different well logs data.
- 3- To evaluate the formation lithology by means of different cross-plots.

- 4- To determine the collapsed area in the wellbore wall and the accompanying entry of the drilling solution and mud inside these voids forming the so-called washout zone, which usually works to hide some of the true properties of the formation. These areas are determined by subtracting the well diameter from the caliber log reading.
- 5- Calculating the percentage of shale within the formation rocks (Vsh) using the following equations:

$$Vsh = 0.083 \times [2^{(3.7 \times IGR)} - 1] \text{ --- (For Tertiary rocks) --- (1)}$$

Where (IGR) is the gamma ray index and can be represented by the following equation

$$IGR = \frac{GRlog - GRmin}{GRmax - GRmin} \text{ --- (2)}$$

Where (GRlog) represents the gamma ray reading, (GRmin) is the minimum gamma ray reading (clean sand or carbonate), (GRmax) is the maximum gamma ray reading (shale line),

- 6- Determining the porosity using each type of available logs (Neutron porosity “NPHI” Density porosity “PHID”, and Sonic porosity “PHIS”)

Where (NPHI) is neutron log’s reading, and

$$PHID = \frac{\rho_{ma} - \rho_{log}}{\rho_{ma} - \rho_f} \text{ --- (3)}$$

$$PHIS = \frac{\Delta t_{log} - \Delta t_{ma}}{\Delta t_f - \Delta t_{ma}} \text{ --- (Wyllie et al., 1956) --- (4)}$$

Where NPHIsh, PHIDsh, PHISsh are neutron porosity, density porosity, sonic porosity of shale respectively. ρ_{ma} (for limestone 2.71 g/cc), ρ_f (for freshwater 1 gm/cc), ρ_{log} are density for matrix, drill fluid density, density log reading respectively. Δt_{ma} (for limestone 47.5 μ sec/ft), Δt_f (for water 189 μ sec/ft), Δt_{log} are transit time for matrix, drill fluid transit time, sonic log reading respectively

- 7- Determining the corrected porosity (corrected neutron porosity “NPHIc”, corrected density porosity “PHIDc”, corrected sonic porosity “PHISc”) according to the following equations:

$$NPHIc = NPHI - (Vsh \times NPHIsh) \text{ --- (5)}$$

$$PHIDc = PHID - (Vsh \times PHIDsh) \text{ --- (6)}$$

$$PHISc = PHIS - (Vsh \times PHISsh) \text{ --- (7)}$$

- 8- Evaluation of the total porosity (PHItotal), secondary porosity (PHIsec) as well as the effective porosity (PHIE) of the formation through the following equations:

$$PHI_{total} = \frac{NPHI + PHID}{2} \text{ --- (8)}$$

$$PHI_{sec} = PHI_{total} - PHISc \text{ --- (9)}$$

$$PHIE = PHI_{total} \times (1 - Vsh) \text{ --- (10)}$$

- 9- Determination sonic waves velocity (IV) of formation rocks using transit time equation as show below:

$$IV(m/s) = (1 / (\Delta t_{log}(\mu. s/ft))) * 3.2808 * 106 \text{ --- (11)}$$

Where the velocity determination is very important in identifying many physical properties such as hardness of rocks and indirectly estimating the porosity of rocks.

Results

Formation lithology

One of the important properties involved in estimating porosity through various well logs is the lithology of formation rocks. The lithology of the formation can be determined by several lithological cross-plots that are created by some physical characteristics, which are recorded by different well logs (Schlumberger, 1991).

Density-Photoelectric Factor (RHOB-PEF) Cross-plot

In identifying the formation lithology, RHOB-PEF is one of the crucial intersection cross-plot. This cross-plot is established for well K-218 only due to the unavailability of an PEF logs in the other wells. Through this cross-plot (Fig. 3), it can be seen that most parts of the formation are located in the area confined between the limestone and dolomite lines, which are closer to the limestone line, which indicates that the formation's lithology is limestone and dolomite limestone. Also, it can be noted that some points are close to the sandstone line, perhaps due to the presence of silica returning to the drilling mud in the areas where the well is washout (The zone is in grey color in fig. 4).

Density-Neutron (RHOB-NPHI) Cross-plot

This cross-plot is established for wells K-218 and K-246 due to the unavailability of a density log for well K-183. From RHOB-NPHI cross-plot (Fig. 5) we can note that many points are located on the limestone line and in the area confined between the limestone and dolomite line, while limited number of points are located in the area confined between the dolomite line and sandstone (silica) line, which may be due to the silica contained in the drilling mud that invades the washout zones, which are especially clear in the lower half of the well K-218 (Fig. 4a). This can also be seen clearly at all formation depths in well K-246 (Fig. 4b), making most of the points in cross plot located near the sandstone line (Fig. 5b).

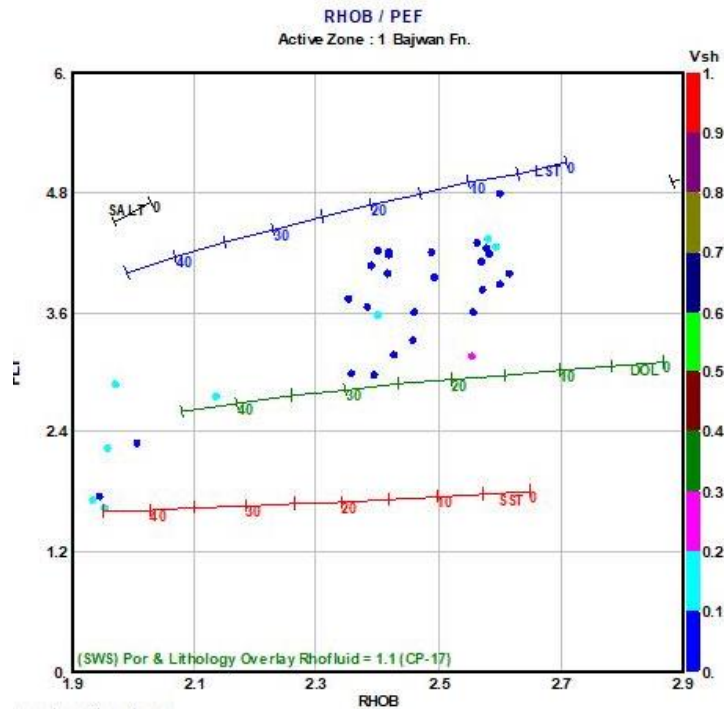


Fig. 3. RHOB-PEF cross plot for well K-218

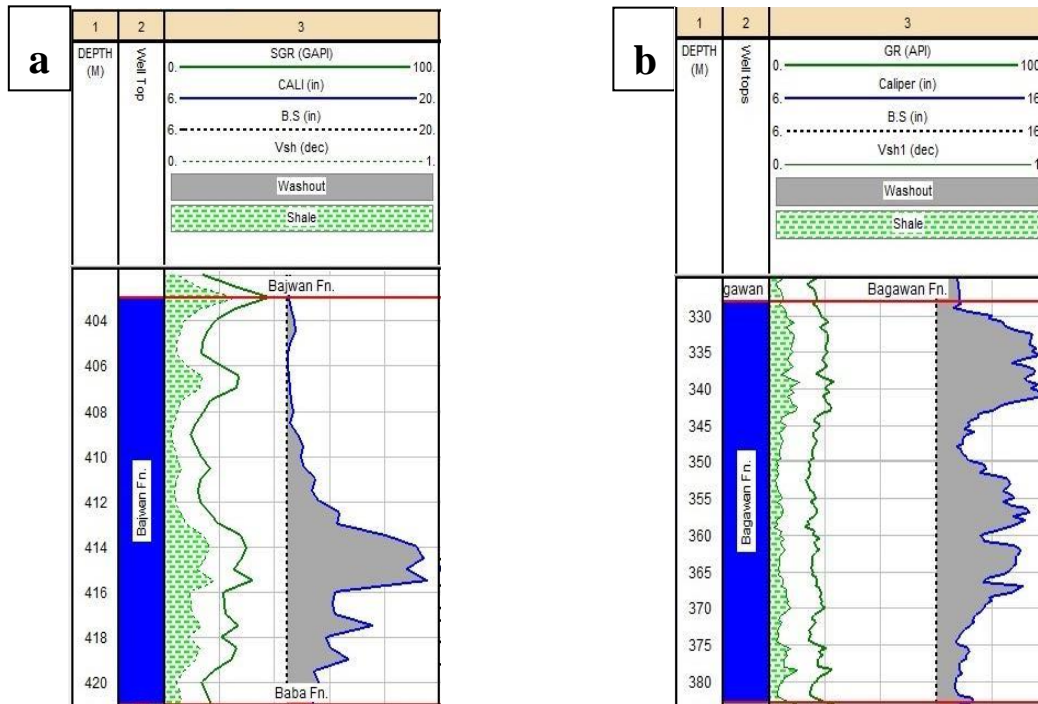


Fig. 4. Washout zones in a: well K-218 b: well K-246

M-N Cross-plot

The M-N cross-plot uses the neutron, density, and sonic logs to identify formation rock minerals, were

$$M = \frac{\Delta t_f - \Delta t_{log}}{\rho_b (\rho_{log}) - \rho_f} * 0.01 \text{ --- (12)}$$

$$N = \frac{NPHI_f - NPHI_{log}}{\rho_b - \rho_f} \text{ --- (13)}$$

Also, this cross-plot is established for wells K-218 and K-246 due to the unavailability of a density log for well K-183.

Figure (6) shows the M-N cross-plot for wells K-218 and K-246. From this cross-plot, it can be seen that at well K-218 (Fig. 6a) the formation is located on the limestone line and slightly deflected to the left of the this plot towards the dolomite, with a few points scattered randomly below and to the right of the drawing due to the effect of the washout zone on the results, and the effect of this washout zone appears clearly in the M-N cross-plot of well K-246 (Fig. 6b), where most of the points appear randomly scattered above and below the plot, due to the effect of the washout on the results.

Density Porosity-Neutron porosity (PHID-NPHI) cross-plot

After the completion of the porosity calculation using the density and neutron logs, a neutron-density porosity cross-plot is created to find out how the shale is present inside the formation rocks. It is shown through this plot that the shale is disseminated within the formation rocks in well K-218 (Fig. 7a) and well K-246 (Fig. 7b). It can also be seen that some points spread in the upper part of the cross-plot for the two wells towards the areas affected by the gas, which indicates that the formation may contain a limited amount of gas.

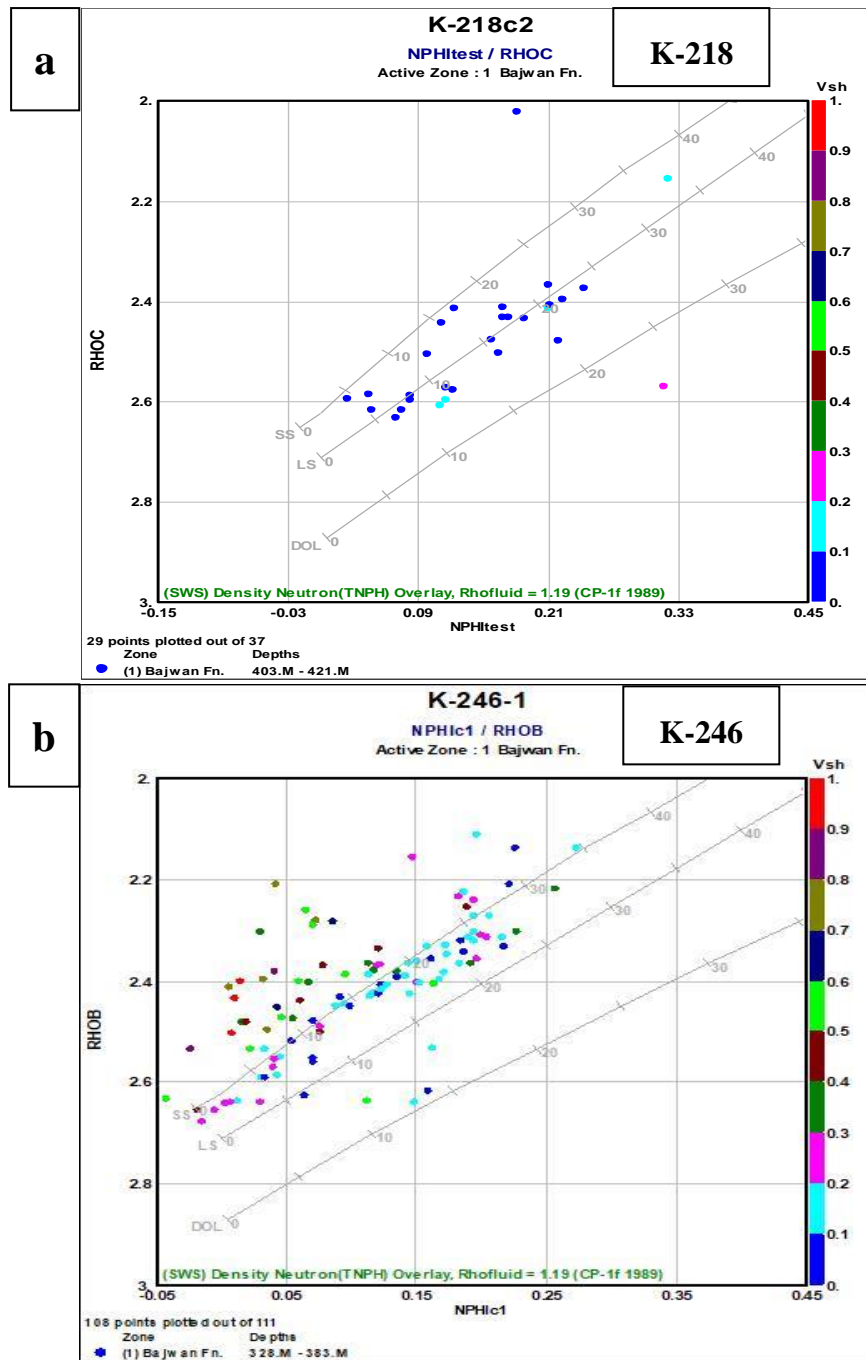


Fig. 5. RHOB-NPHI Cross-plot of wells a: K-218 b: K-246

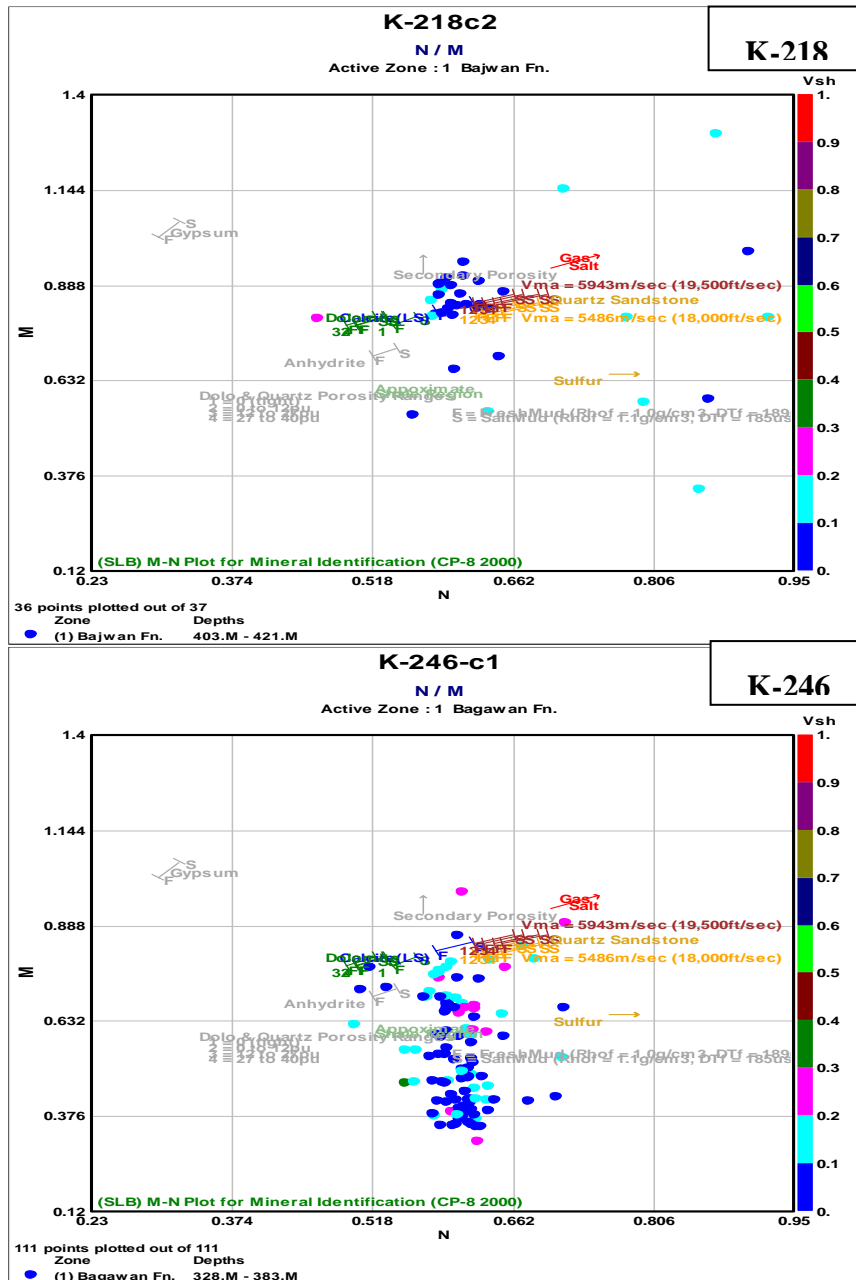


Fig. 6. M-N Cross-plot of wells a: K-218 b: K-246

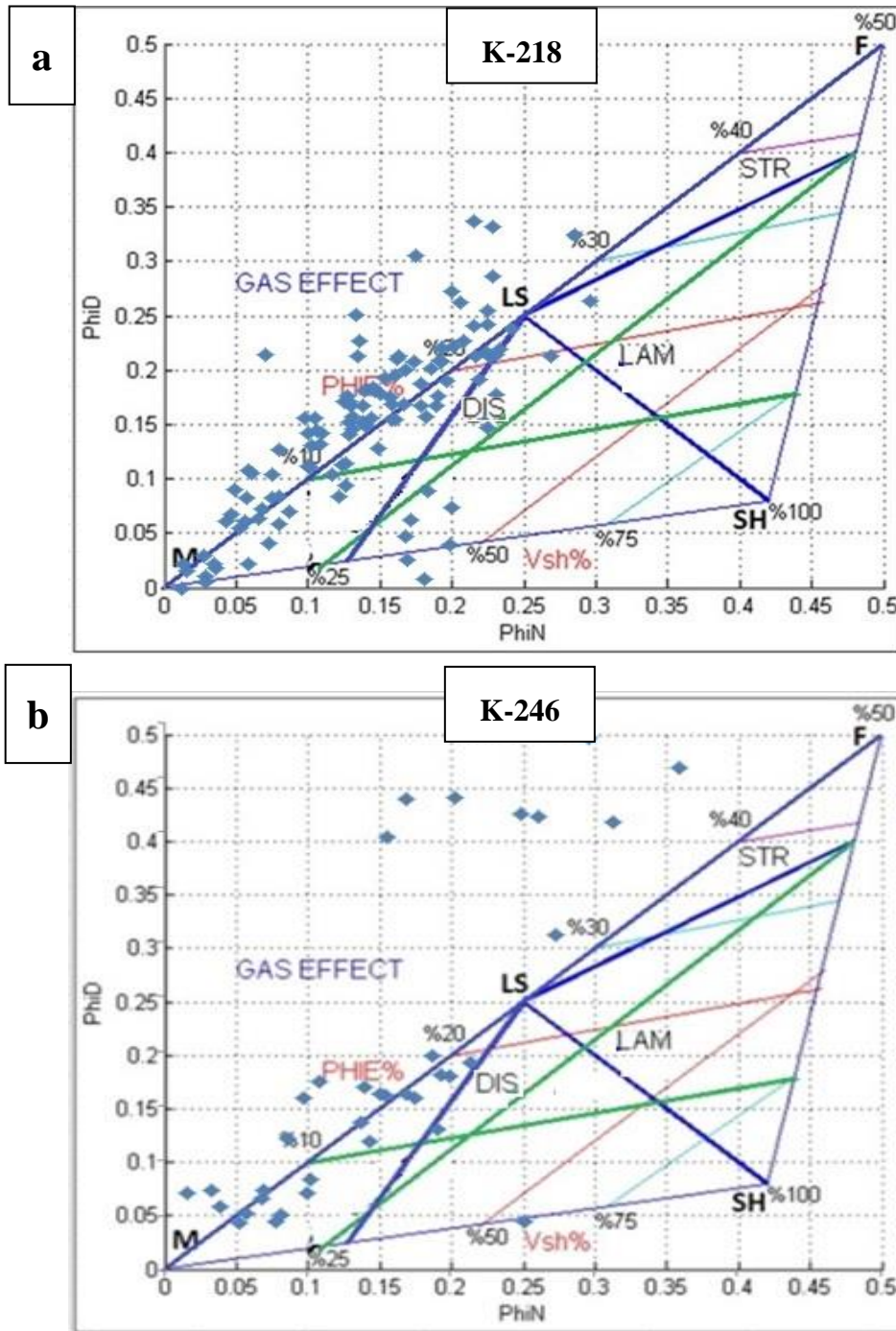


Fig. 7. PHID-NPHI cross-plot

Gama ray-Neutron porosity minus Density porosity (GR-NPHI minus NPID) plot

This plot represents the relationship between the intensity of the gamma ray on the x-axis and the the neutron porosity minus the density porosity on the y-axis. There are several purposes for this plot, one of the most important of these purposes is to determine the effect of gas on formation rocks.

The results given in figure (8) show that there are some points in the part of influence of gas (the lower part of the plot), which supports the possibility of the presence of gas in the rocks of this formation.

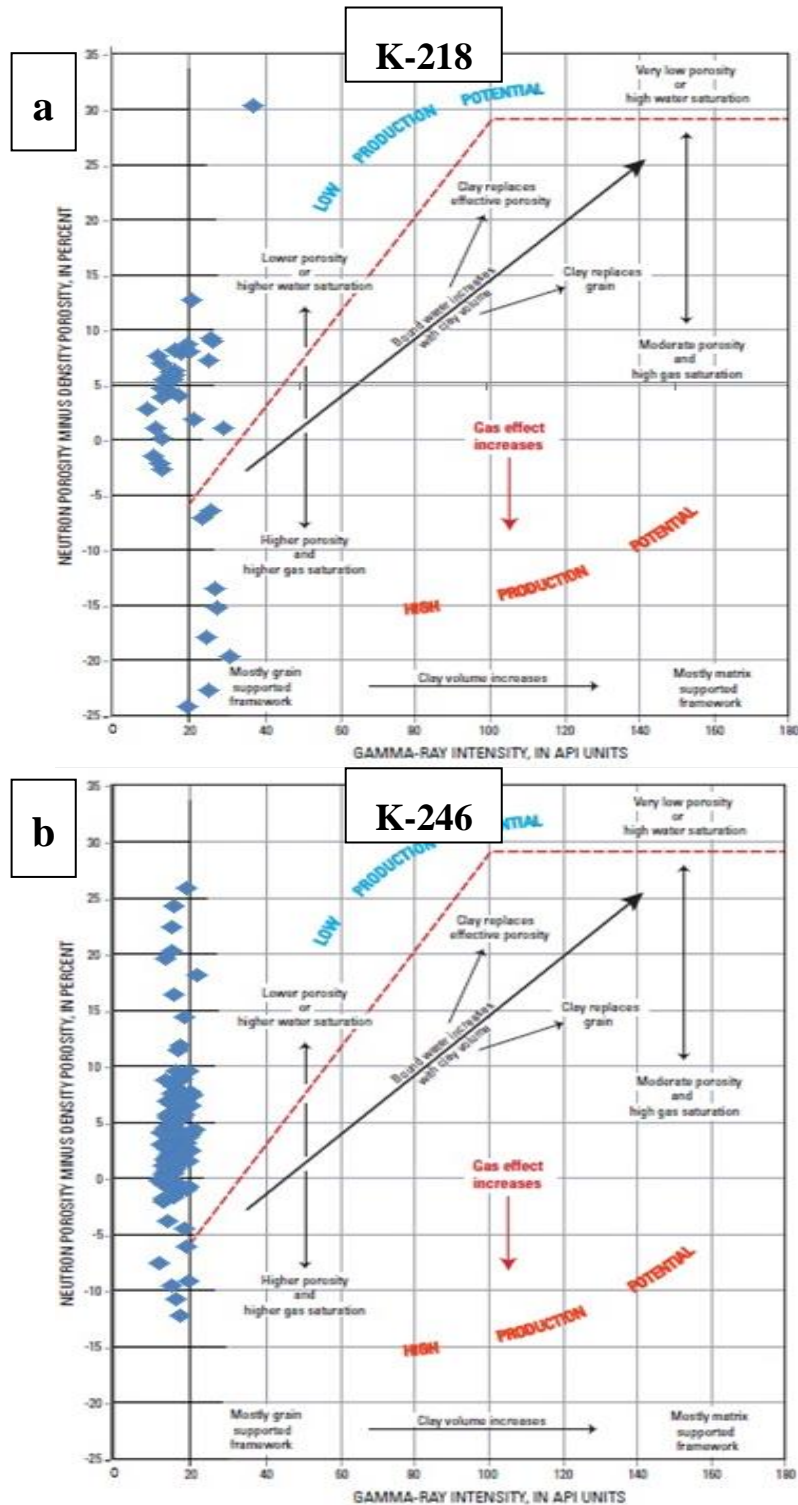


Fig. 8. GR-NPHI minus NPID plot for wells a: K-218 b: K-246

Porosity

According to their origin, pores in carbonates are generally divided into two main groups primary and secondary (Choquette and Pray, 1970). Primary porosity, also known as depositional porosity, is created as the sediment was being deposited including many types, the most important interparticle, intraparticle, fenestral, and shelter. Secondary porosity refers to porosity that develops as a consequence of post-depositional diagenetic changes to the rock, which frequently involve both dissolution and cementation. One of the most important types are vuggy, fracture, channels, stylolitic, cavernous, and destructive intercrystalline pore form for fabrics. It should be observed that a primary porosity can be increased by dissolution and early dolomitization or decreased by cementation to create a secondary porosity in an initial pore.

Since post-depositional burial cementation and compaction often significantly decrease primary porosity in carbonate rocks, most pore types in carbonates are secondary in origin (Halley and Schmoker, 1983; Mazzullo et al. 1992). The outliers are those primary pores that have been preserved because of early-stage hydrocarbon accumulation (Feazel and Schatzinger, 1985)

The types of porosity are studied and analyzed by two methods: thin sections of rock cutting and analysis of available well logs (neutron, density, and sonic logs).

Thin sections

Twenty thin sections of the Bajawan Formation are examined at various depths in the three studied wells, and numerous forms of primary and secondary porosity are found as shown below:

In the well K-183, several types of primary porosity (interparticle and intraparticle porosity) and secondary porosity (channel, fractures, cavern, vuggy, and fenestral porosity) have been observed as shown in figure (9). As for the thin sections of well K-218, also several types of primary porosity (interparticle, intercrystal, and intraparticle porosity) and secondary porosity (channel, carven, and vuggy porosity) have been observed (Fig. 10). In well K-246 have been observed the main two types of porosity; primary (intraparticle porosity) and secondary (vuggy, channel, cavern, and fenestral porosity) as shown in figure (11).

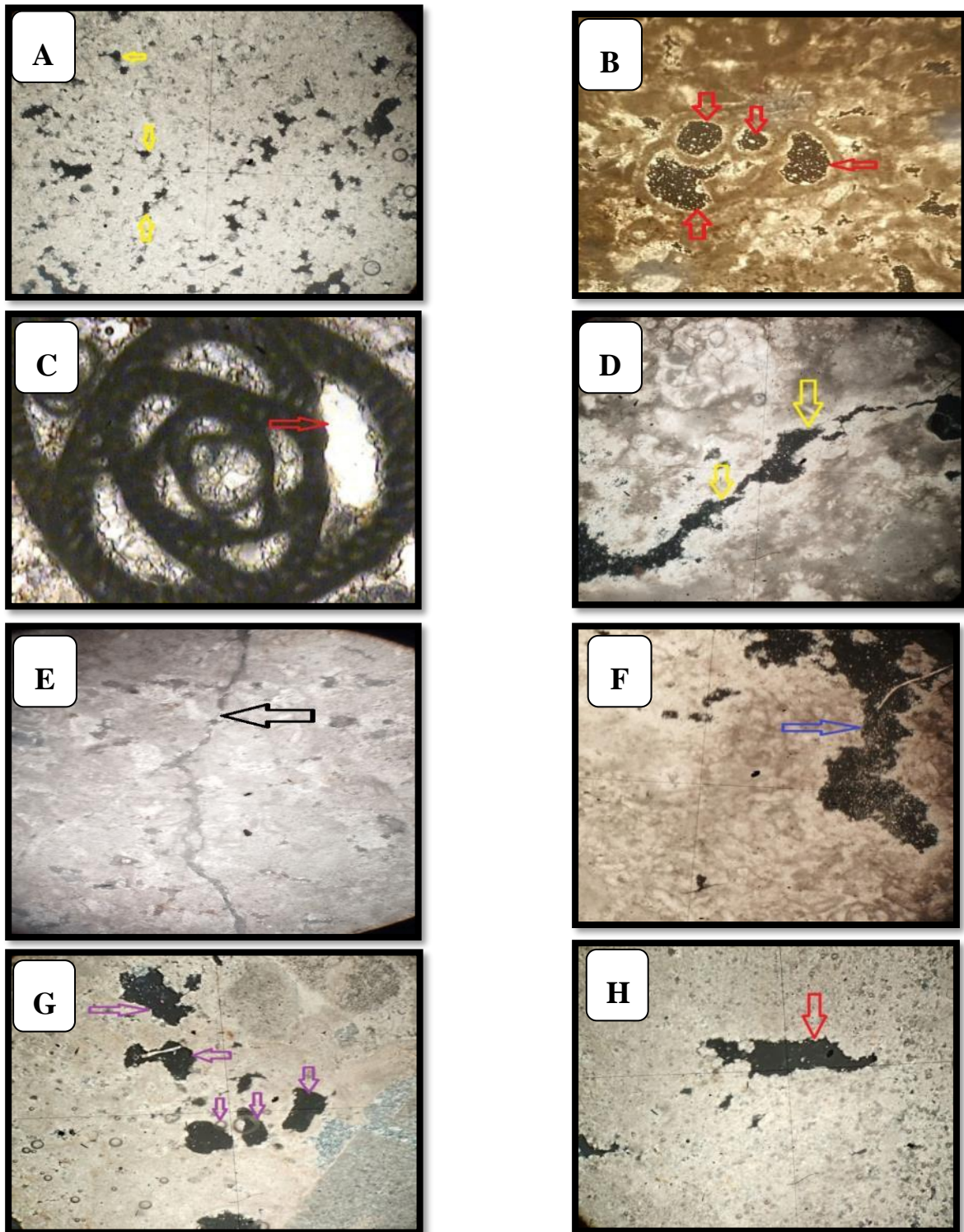


Fig. 9. Photomicrographs of eight samples from well k-183 showing the major porosity types in Bajawan Formation where the yellow arrow points; A. Interparticle porosity at depth 873 m., B. Intraparticle porosity at depth 902 m.; C. Intraparticle porosity at depth 906 m.; D. Channel porosity at depth 890 m.; E Fracture porosity at depth 902 m.; F. Cavren porosity at depth 886 m.; G. Vuggy porosity at depth - 873 m.; H. Fenestral porosity at depth 876 m.

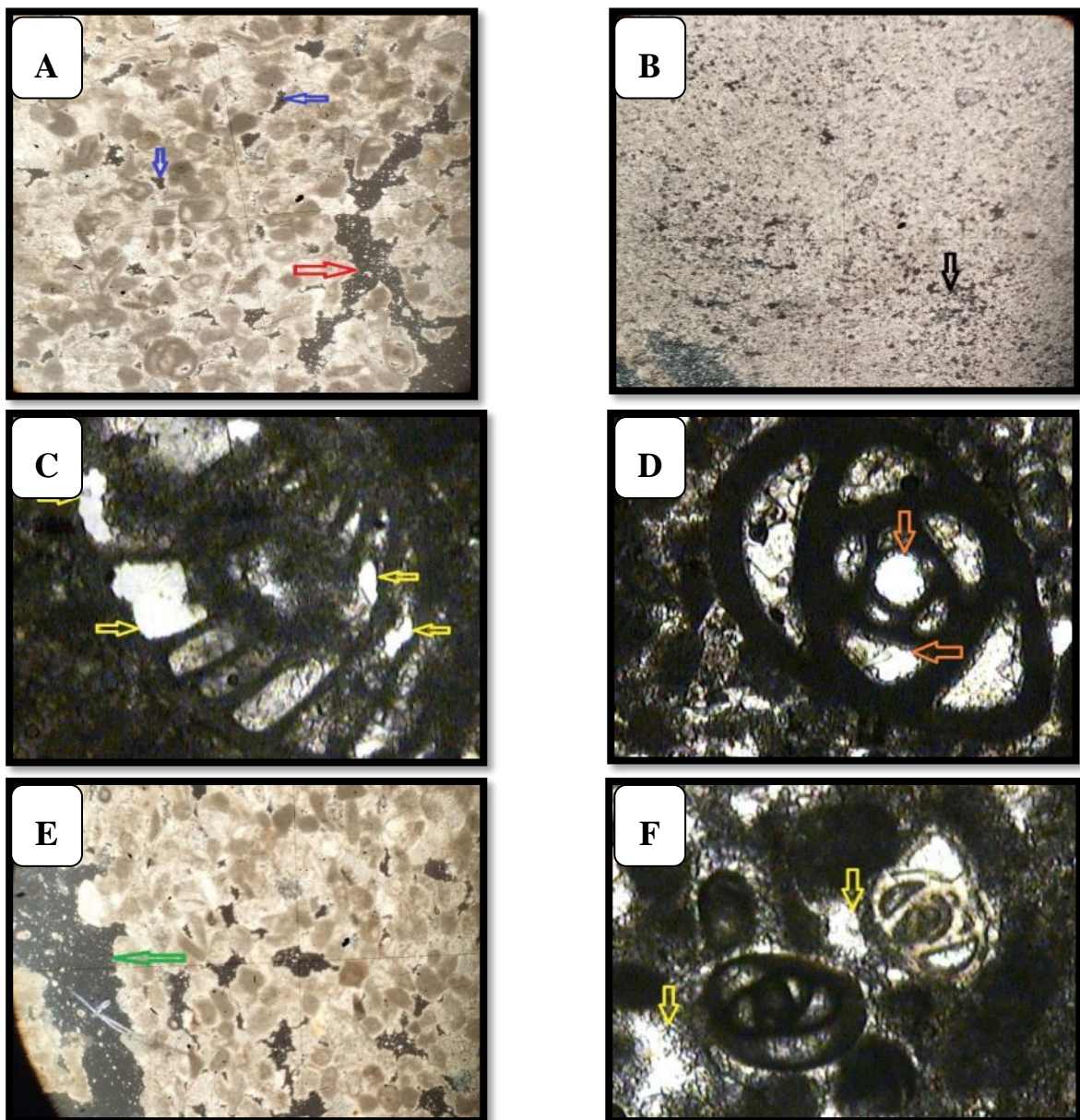


Fig. 10. Photomicrographs of six samples from well k-218 showing the major porosity types in Bajawan Formation where the yellow arrow points A. Interparticle porosity (blue arrows), and channel porosity (red arrow) at depth 403 m.; B. Intercrystal porosity at depth 417 m.; C. Intraparticle porosity at depth 419 m.; D. Intraparticle porosity at depth 418 m.; E. Carven porosity at depth 403 m.; F. Vuggy porosity at depth 404 m.

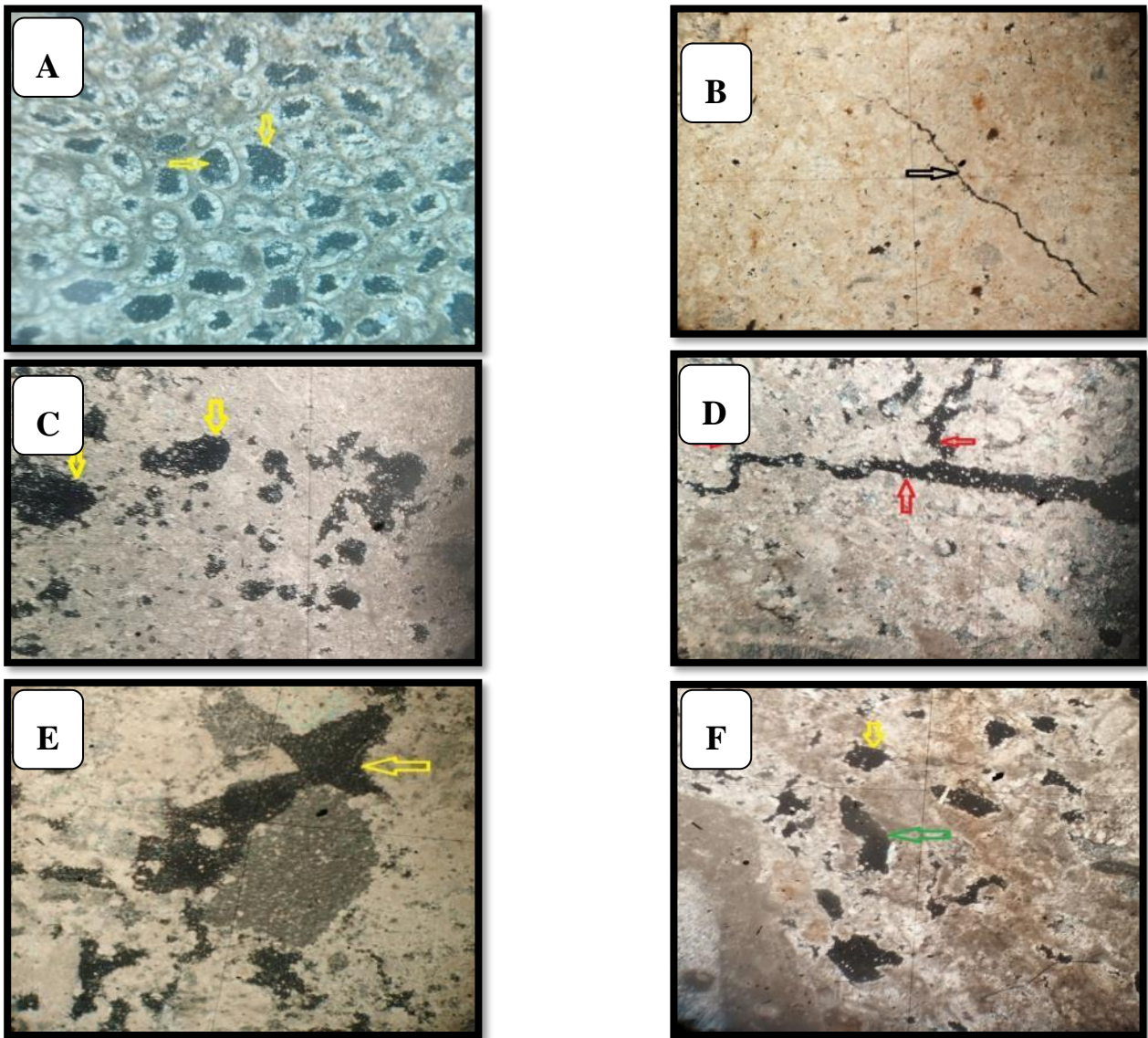


Fig. 11. Photomicrographs of six samples from well k-246 showing the major porosity types in Bajawan Formation where the yellow arrow points: A. Intraparticle porosity at depth 334 m.; B. Fracture porosity at depth 349 m.; C. Vuggy porosity at depth 329 m.; D. Channel porosity at depth 350 m.; E. Cavern porosity at depth 328 m.; F. Fenestral porosity (green arrows), Vuggy porosity (yellow arrow) at depth 335 m.

Well logs analysis

Well K-183

The results of this well (Fig. 12) show that the formation contains a small volume of shale and high secondary porosity compared to the primary porosity.

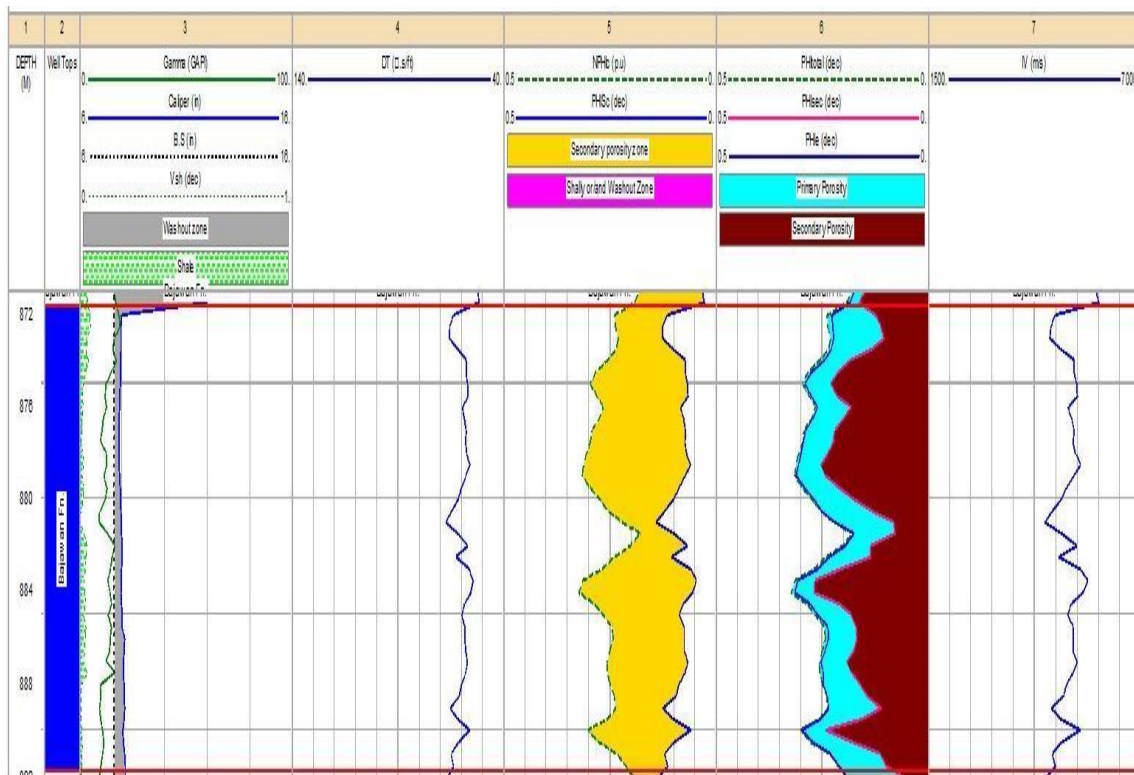


Fig. 12. Results of analysis of well K-183 logs: The yellow shaded area in track 5 and maroon shaded area in track 6 represent the secondary porosity zone (when $NPHi_c$ greater than $PHISc$) and aqua shaded area in track 6 represents the primary porosity zone (where $PHI_{primary} = PHISc$)

Well K-218

Figure (13) shows the results of analyzing different well logs. It can be seen that the washout zones are extended widely at the lower parts of the formation (spatially between the two depths 412-416 m). According to the analysis and interpretation of the well logs data, the volume of shale ranges between 2 - 25%. Also, we can notice some secondary porosity zones, especially below the depth of 218 m. and to a lesser extent at depths 403-406 m.

There are some indications of a possible presence of gas within the regions of high NPHI and low PHID zones at the depths 405 and 409 m.

Well K-246

At well K-246, the washout zones are extended along the depth of the formation (Fig. 14), and thus the results of the porosity calculation are inaccurate because the different types of porosities calculated from the well logs are greatly affected by the drilling solution that invades these zones.

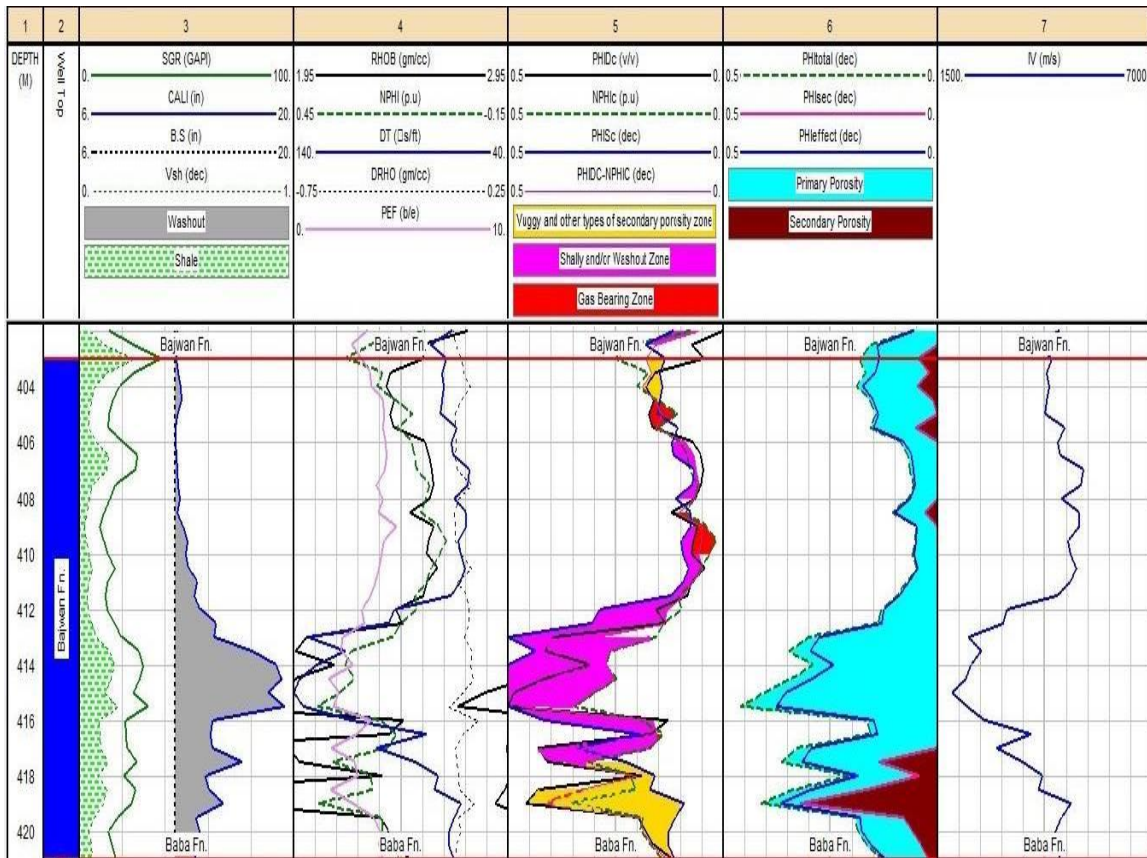


Fig. 13. Results of analysis of well K-218 logs

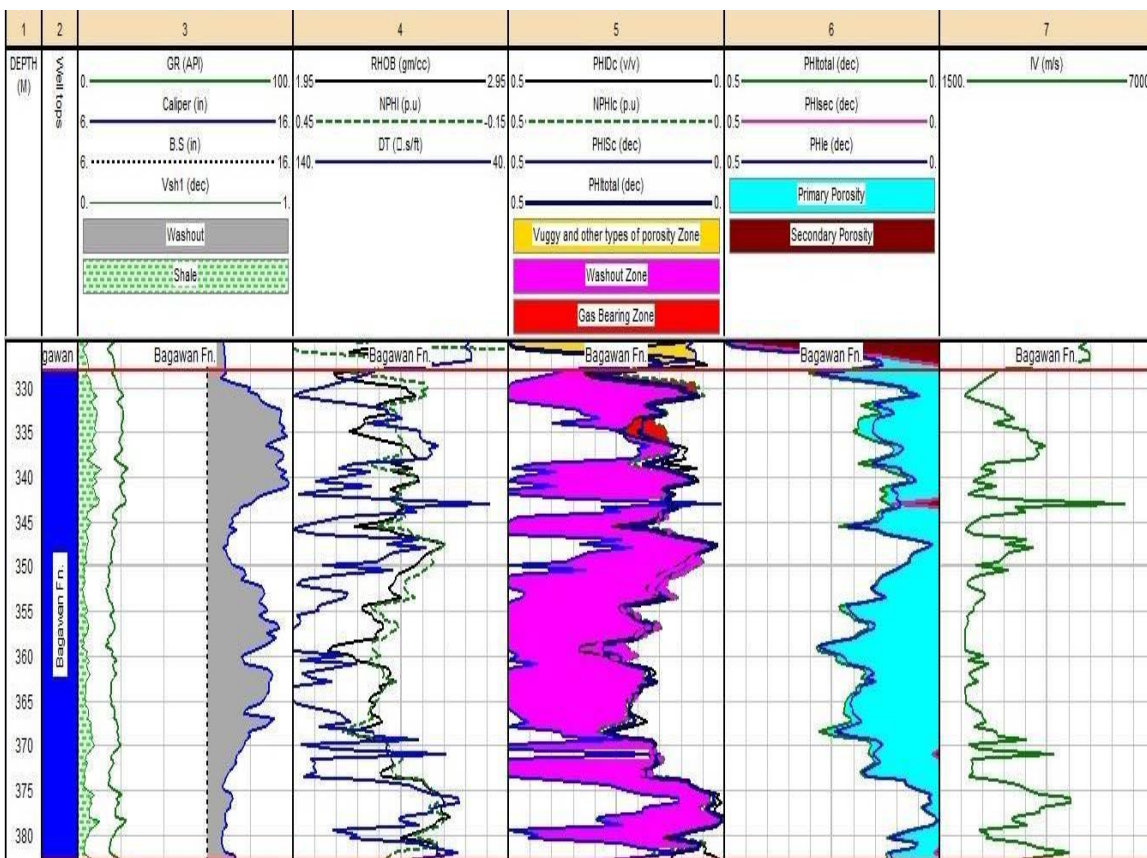


Fig. 14. Results of analysis of well K-246 logs

In general, the rates of shale percentage and the percentage of porosity types shown in table 3:

Table 3 : The average values of the shale percentage, the average of the types of porosity, and the velocity of the acoustic waves of the formation in studied wells

Well	Property rate					Seismic velocity (IV'm/sec')
	Shale percentage rate (Vsh%)	Total porosity (PHItotal%)	Primary porosity (PHIS%)	Secondary porosity (PHIsec%)	Effective porosity (PHIE%)	
K-183	2	26	9.3	16.7	25.5	5133
K-218*	7.7	14.6	11.7	2.9	13.2	4002
K-246	5.6	14.7	14.6	0.1	13.2	2958

* The values are calculated after ignoring the greatest washout zone in well K-218 (412-416 m.), which may cause inaccurate results for formation properties.

Discussion

The porosity of the Bajawan Formation is one among the most significant petrophysical characteristics that must be calculated for the seek of development of hydrocarbon extraction operations in the Baba field.

Lithological cross-plots of the three wells (K-183, K-218, and K-246), as shown in figures (3, 5, and 6) indicate that the formation lithology is generally composed of limestone and dolomitic limestone with a small percentage of silica, which increases at the washout zones. These areas were invaded by drilling mud that contains a high percentage of silica.

Shale volume in the three wells is low (not exceeding the average of this percentage 7.7%), which indicates the sedimentary environment was shallow. In addition to the lack of clastic sources, and it is consistent with the environmental studies of the formation accomplished by many authors (Jassim and Goof, 2006; Ghafur, 2015; Farhan, et al, 2016), which confirms that the formation was deposited in back-reefs environment.

The formation porosity in the three studied wells includes the primary porosity formed during the sedimentation that is inferred from the sonic log's information, as appeared in all parts of the three wells (Fig. 12, 13, 14) and thin section (Fig. 9A, B, C; 10A, B, C, D; 11A). This porosity represents the true primary porosity of the formation at the whole formation depths of well K-183. It also represents the true primary porosity in the upper half of the formation in well K-218 that is not affected by washout compared to well K-246, where all formation is affected by washout.

The washing process led to an increase in the percentage of primary porosity at the expense of secondary porosity due to the penetration of drilling mud in the washout area because this mud has a high percentage of the primary porosity as most of the porosity calculated is due to the drilling mud, which led to the concealment of the real information of porosity.

If we ignore the washout areas in the three wells of the study, we can notice that the primary porosity values range between 1 - 20% with a rate of 5.9%.

The other type of porosity of the Bajawan Formation is secondary porosity, which is formed after sedimentation as a result of various diageneses processes that may increase or decrease the primary porosity. This type of porosity in its various forms is observed in the Bajawan Formation which has been identified by the thin sections (Fig. 9D,E,F,G,H; 10A,E,F; 11B,C,D,E,F), as it is calculated from the logs data of wells K-183 (Fig. 12) and K-218 (Fig. 13) in its upper part, and it could not be calculated in well K-246 due to the dominance of the primary porosity of the drilling mud as a result of the influence of all parts of the formation by washing areas.

Secondary porosity of the formation areas unaffected by washout is between 5 - 23% with a rate of 10.8 %.

The effective porosity of the formation, which includes connected pores, whether primary or secondary, is close to total porosity because the formation has a low volume of shale. It is between 6 and 31% in regions not affected by washout with an average rate of 19.4%.

Some of the results from the analysis of the cross-plots (Figs. 7, 8) show that some parts of the formation may be affected by the presence of gas, what reinforced this is the analysis of K-218 well logs, which supports the possibility of gas presence at depths of 405 and 409 m (Fig. 13), where the NPHI is less than the PHID, and this also appears in well K-246 at a depth of 335 m (Fig. 14), but It is not reliable because the well was affected by washout. This possibility is reinforced by the presence of the Fatha Formation above the Bajawan Formation, which represents the cap rocks.

By analyzing the velocity of the sonic waves calculated from the sonic logs of three logs, it is observed that the rate of this velocity in the areas unaffected by washout range between 4002 - 5133 m/sec, which is an ideal velocity for porous dolomite limestone rocks (Lowrie, 2007). It is also noted that this velocity decreases significantly in the washout areas, where its rate reached approximately 2958 in well K-246, and this also applies to depths affected by washout in the lower half of well K-218, where the velocity of sonic waves decreased to approximately 2000 m/s in this part.

Conclusion

By analyzing and comparing the well logs information and the information of the thin section, the current study reached several conclusions worthy of attention, which can be summarized as follows:

- Low percentage of shale in the Bajawan Formation indicating that the sedimentary environment of the formation was shallow, in addition to the possible lack of a clastic sources.
- The percentage of the effective porosity in the formation rocks is relatively high, which may help in re-development of wells produced from this formation.
- Most of the types of primary and secondary porosity are observed in the formation rocks through the thin sections analysis, and this is supported by the percentage of these types when analyzing the well logs.
- The presence of some areas in the formation that may contain gas between the pores of its rocks.
- The velocity of the sonic waves of the formation rocks is within the range of the sonic wave velocity of porous dolomitic limestone.
- Washout zones cause some errors in calculating the types of porosity, especially the secondary porosity, which is usually obscured as a result of the dominance of the primary porosity of the drilling mud.

Acknowledgements

Many thanks go to the University of Mosul, College of Science for offering the facilities helped raise the caliber of this effort.

References

- Abdulaziz, A.M., Ali, M.K., Hafad, O.F., 2022. Influences of Well Test Techniques and Uncertainty in Petrophysics on Well Test Results, *Energies* 2022, 15, 7414. DOI: [org/10.3390/en15197414](https://doi.org/10.3390/en15197414).
- AL-Hamdany, A.M., Sulaiman, M.A., 2014. Porosity of Avanah Formation and its Stratigraphical Distribution in Selected Wells of Kirkuk Oil Field, *Iraqi National Journal of Earth Science*, V.14, No.1, pp.49-66, (In Arabic).
- Al-Juraisy, B.A. and Al-Majid, M.H.A., 2021. Importance of velocity deviation technique and negative secondary porosity in detection of hydrocarbon zones in Khasib formation, east Baghdad oil field. *The Iraqi geological journal*, 54(2E), 86-103pp. DOI: [DOI:org/10.46717/igj.54.2E.6Ms-2021-11-22](https://doi.org/10.46717/igj.54.2E.6Ms-2021-11-22)
- Al-Majid, M.H, 2019. New petrophysical equations for Hartha-Tannuma interval in the East Baghdad Oil Field, *Iraqi National Journal of Earth Science*, 2(19), 136-152. DOI: [10.33899/earth.2019.170285](https://doi.org/10.33899/earth.2019.170285)
- Al-Majid, M.H.A, 2021. Petrophysical properties estimation of euphrates reservoir in qayyarah oil field using core and well log data. *Iraqi geological journal*, 54(2e), pp. 186–197. DOI: [DOI: org/10.46717/igj.54.2E.13Ms-2021-11-29](https://doi.org/10.46717/igj.54.2E.13Ms-2021-11-29)
- Bellen, R.C. Van., 1956. The stratigraphy of the main Limestone of Kirkuk, Bai Hassan and Qarah Chaugh Dagh structures in Northern Iraq. *Inst. Petroleum Found.*, Vol.42, London.
- Bellen, R.C.V, Dunnington, H.V., Wetyzel, R. and Morton, D., 1959. *Lexique stratigraphique international*, Asia, Iraq, Vol. 3C, 10a, 333 p.
- Buday, T., 1980. *The Regional Geology of Iraq. Vol. 1: Stratigraphy and Palaeogeography*. Publications of GEOSURV, Baghdad, 445p.
- Choquette, P.W. and Pray, L.C., 1970. Geologic nomenclature and classification of porosity in sedimentary carbonates: *AAPG Bulletin*, v. 54, pp. 207-250.
- Ditmar, V.I., Begishev, F.A., Afanasia, J.T., Befousova, M.G., Briousov, B.A., Petchernikov, V.V., Cheremnyh, E.M., Shmakova, E.L., Koverznev, V.Y. & Nazarov, N.P., 1971. *Geological condition & hydrocarbon prospects of the republic of Iraq (Northern & Central parts)*. Rep. INOC Library, Baghdad.
- Farhan, H.N., Kadem, L.S., Mohammed, Q.A., 2016. Microfacies and depositional environment of Bajawan and Baba Formations in Kirkuk Oil fields north Iraq, *Tikrit Journal of Pure Science*, 21 (6), pp. 112-125, DOI: [DOI: DOI: org/10.25130/tjps.v21i6.1089](https://doi.org/10.25130/tjps.v21i6.1089)
- Feazel, C.T. and Schatzinger, R.A., 1985. Prevention of carbonate cementation in petroleum reservoirs, in N. Schneidermann and P.M. Harris, eds., *Carbonate Cements: SEPM Special Publ.* 36, p. 97-106.
- Fouad, S., 2015. "Tectonic map of Iraq, scale 1: 1000 000", 3rd. edition. *Iraqi, Iraqi Bulletin of Geology and Mining* Vol.11, No.1, p 1 – 7.
- Ghafur, A.A., 2015. Integrated depositional model of the Carbonate Kirkuk Group of Southern Kurdistan-Iraq, *Journal of Natural Sciences Research*, Vol.5, No.24, pp.79-106
- Halley, R.B. and Schmoker, J.W., 1983. High porosity Cenozoic carbonate rocks of south Florida: progressive loss of porosity with depth: *AAPG Bulletin*, v. 67, p. 191-200.

- Hou, J., Zhao, L., Zeng, X., Zhao, W., Chen, Y., Li, J., Wang, S., Wang, J., Song, H., 2022. Characterization and Evaluation of Carbonate Reservoir Pore Structure Based on Machine Learning, *Energies*, 15, 7126. [DOI: org/10.3390/en15197126](https://doi.org/10.3390/en15197126).
- Jassim, S.Z. and Goff, J.C., 2006. *Geology of Iraq*. 1st Edition, published by Dolin, Prague and Moravian Museum, Brno, Printed in the Czech Republic, 341p.
- Khudhair, M. H. and Al-Zaidy, A.A., 2018. Petrophysical properties and reservoir development of Albian succession in Nasiriyah oil field , Southern Iraq, *Iraqi Bulletin of Geology and Mining* , Vol.14, No.2, 2018, p 61 – 69
- Lowrie W., 2007. *Fundamentals of Geophysics*. 2 nd edition, Cambridge University Press, 381p.
- Mahdi, Z.A. and Farman, G.M., 2023. Estimation of Petrophysical Properties for Zubair Reservoir in Abu-Amood Oil Field, *Iraqi Geological Journal*, 56 (1B), 32-39, [DOI: 10.46717/igj.56.1B.3ms-2023-2-11](https://doi.org/10.46717/igj.56.1B.3ms-2023-2-11).
- Mazzullo, S.J. and Chilingarian, G.V., 1992. Diagenesis and origin of porosity, in G.V. Chilingarian, S.J. Mazzullo, and H.H. Rieke, eds., *Carbonate Reservoir Characterization: A Geologic-Engineering Analysis, Part I*: Elsevier Publ. Co., Amsterdam, *Developments in Petroleum Science* 30, p. 199-270.
- Mehdi, A., 2018. *Iraqi Oil: industry evolution and short and medium-term prospects*, OIES PAPER: WPM 79, Oxford Institute for Energy Studies, Registered Charity, No. 286084, 36p, [DOI: org/10.26889/9781784671211](https://doi.org/10.26889/9781784671211).
- Schlumberger, 1991. *Log Interpretation Principles / applications*. Houston, Tx: Schlumberger Educational Services.
- Wyllie, M.R., Gregory, A. R, Gardner, G. H. F., 1956. Elastic wave velocities in heterogeneous and porous media. *Geophysics*, 21(1), 41–70.